Enhanced dielectric properties in single crystal-like $BiFeO_3$ thin films grown by flux-mediated epitaxy

S.-H. Lim, M. Murakami, J. H. Yang, S.-Y. Young, J. Hattrick-Simpers, M. Wuttig, L. G. Salamanca-Riba,[a] and I. Takeuchi[b]
Department of Materials Science and Engineering, University of Maryland, College Park, Maryland 20742, USA

(Received 5 October 2007; accepted 14 December 2007; published online 8 January 2008)

We have fabricated single crystal-like $BiFeO_3$ (BFO) thin films by flux-mediated epitaxy using pulsed laser deposition (PLD). The Bi–Cu–O flux composition and its thickness were optimized using composition spread, thickness gradient, and temperature gradient libraries. The optimized BFO thin films grown with this technique showed larger grain size of ~2 μm and higher dielectric constant in the range of 260–340 than those for standard PLD grown films. In addition, the leakage current density of the films was reduced by two orders of magnitude compared to that of standard PLD grown films. © *2008 American Institute of Physics*. [DOI: 10.1063/1.2831665]

Multiferroic $BiFeO_3$ (BFO) thin films are widely studied because of their antiferromagnetic and ferroelectric ordering well above room temperature.[1–4] In pursuing their device applications, it is critical to address and control their microstructural variation and the relatively large leakage current primarily due to the high volatility of Bi and heteroepitaxial constraints imposed by the substrate. The strain in the films together with the evaporation of bismuth can produce Bi deficient secondary phases such as antiferromagnetic α-Fe_2O_3, and ferromagnetic γ-Fe_2O_3 and Fe_3O_4 which form to compensate the local imbalance in chemical composition and structural distortion.[5–8]

In our previous work, we observed enhancement of strain relaxation and magnetization in Bi–Fe–O films that contained α- and γ-Fe_2O_3 phases.[6,7] Bismuth deficiencies and oxygen vacancies are known to induce significant leakage current density by forming impurity energy levels in the bandgap.[9,10] Many attempts have been made to improve the crystallinity and enhance the properties of BFO thin films by different growth techniques.[11,12] However, the films frequently have high densities of defects because of the high growth temperature required in these techniques. In this work, we report a substantial improvement of leakage current and dielectric properties ($\varepsilon \approx 260-340$) in single crystal-like BFO films grown by flux-mediated epitaxy (FME).

In the FME method, an oxide flux on the surface of the film plays a key role in improving the crystallinity of complex oxide films.[13] The vapor ablated from the target material by a pulsed laser meets the flux on the surface of the substrate, diffuses into the liquid intermediate phase and finally solidifies on a predeposited seed layer. The liquid phase (flux) prevents direct deposition of the vapor phase on the solid surface and improves crystallinity. Compared to pulsed laser deposition (PLD), in the FME method, there is enhanced diffusion of the surface atoms in the flux above the quasimelting temperature ($\sim 0.5T_m$), which leads to film growth in equilibrium even at high growth rates.[13–15]

In this work, BFO thin films were grown on $SrRuO_3$ (SRO) buffered (001) oriented $SrTiO_3$ (STO) substrates by standard PLD and by FME for comparison. We ablated a 10% Bi excess $Bi_{1.1}FeO_3$ target with a KrF excimer laser ($\lambda = 248$ nm) at 650 °C and 20 mTorr oxygen partial pressure. Under these conditions, the PLD grown films showed a pure BFO phase. For the FME growth, a mixture of Bi_2O_3 and CuO was selected for the flux material as explained below. The films were characterized using scanning x-ray microdiffraction (XRD), atomic force microscopy (AFM), and transmission electron microscopy (TEM). For the electrical measurements, Pd (100 nm) and epitaxial SRO (50 nm) layers were used as top and bottom electrodes, respectively.

The schematic in Fig. 1(a) shows the deposition procedure for the combinatorial library used to optimize the composition, temperature, and thickness of the Bi_2O_3-CuO flux. The typical library chip size was 9 mm × 4mm. The oxygen partial pressure for the growth of the FME-BFO film was varied in the range of 0.05–1 Torr. A BFO seed layer (~10 nm) was deposited at 650 °C and 30 mTorr oxygen

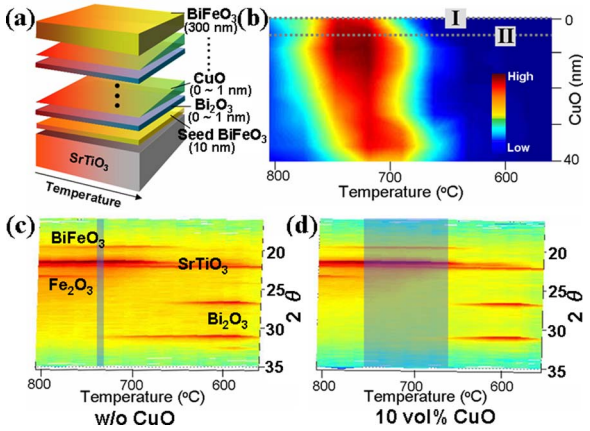

FIG. 1. (Color online) (a) Schematic of the deposition procedure for temperature gradient (580–810 °C) and composition spread experiment. The composition spread consisted of Bi_2O_3 (40 nm) and CuO (0–40 nm). (b) XRD map of spread showing the intensity of the BFO (001) peak as a function of substrate temperature and CuO flux composition (thickness). (c) XRD map in the region marked I in (b) for 0% CuO. (d) XRD map for the region with 10 vol % CuO [labeled II in (b)] with the highest intensity of the BFO (001) peak. The shaded region in (d) shows an enlargement of the growth window of BFO compared to that for films deposited without CuO (c).

[a]Electronic mail: riba@umd.edu.
[b]Electronic mail: takeuchi@umd.edu.

partial pressure before depositing the flux material to lead to growth of BFO. After increasing the temperature to 730 °C, a Bi_2O_3 layer (~1 nm) and a CuO layer (~1 nm) were deposited in an alternating manner to induce interdiffusion between the layers and to prepare a layer with a gradient in composition of the flux. The total thickness of Bi_2O_3 was fixed to 40 nm. Using a moving shadow mask in the PLD chamber during the deposition of CuO, a layer with a thickness gradient was achieved. These conditions gave rise to regions with different ratios of Bi_2O_3/CuO in the flux which varied from pure Bi_2O_3 (without CuO) to $(Bi_2O_3)_{0.5}$–$(CuO)_{0.5}$. In addition, a temperature gradient from 560 to 805 °C was achieved on the substrate over a distance of 9 mm by heating one side of the sample stage using a semiconductor laser. Following the deposition of the flux, a 300 nm thick BFO thin film was deposited on the flux layer.

Figure 1(b) shows the intensity map of the (001) BFO diffraction peak as a function of position of the sample which corresponds to changes in CuO layer thickness (0–40 nm) and the sample growth temperature. The highest intensity of the (001) BFO peak was observed in the region with CuO thickness of 0.4–17 nm and temperature of 710–750 °C. To understand the effect of CuO on the Bi based flux growth, temperature dependent XRD spectra in the regions with 0 vol % CuO [line I in Fig. 1(b)] and ~4.5 nm thick CuO (10 vol % CuO) [line II in Fig. 1(b)] are compared in Figs. 1(c) and 1(d), respectively. The regions with pure Bi_2O_3 flux show a strong Bi_2O_3 XRD intensity peak over a large range of temperatures below 730 °C. This region overlaps with the temperature range for Fe_2O_3 growth [see Fig. 1(c)]. Figure 1(d) shows that addition of 10 vol % CuO in the flux plays an important role, namely, CuO decreases the melting temperature of the Bi_2O_3–CuO flux material thereby suppressing the precipitation of Bi_2O_3. Furthermore, the amount of Bi_2O_3 melt in the flux compensates for evaporated Bi thus suppressing the formation of Fe_2O_3.[16] The comparison of the shadow areas in Figs. 1(c) and 1(d) illustrates the enlarged growth window of BFO for a flux with 10 vol % CuO. Following the combinatorial optimization, a BFO thin film was grown by FME using the optimum flux composition (10 vol % CuO) and the optimized growth temperature (730 °C).

The AFM image in Fig. 2(b) shows dramatically increased grain size (~2 μm) for the FME grown BFO film, which is more than ten times larger than the grain size for films grown by standard PLD [shown in Fig. 2(a) with typical grain size of 50–200 nm]. The height profile of the FME grown BFO film [Fig. 2(c)] shows a fairly smooth surface (compared to the standard PLD grown BFO films) with an average step height of ~1.2 nm, which corresponds to three unit cells of BFO [see inset to Fig. 2(c)]. The width of the terraces varies in the range from 70 to 100 nm.

A cross-sectional bright field TEM image (top) and high resolution images (bottom) of the FME grown BFO film in Fig. 3 exhibit epitaxial growth with very sharp interfaces and smooth surface of the BFO film. In the large area view [Fig. 3(a)], the film grown by FME shows single crystal-like BFO film without grain boundaries, and we see no evidence of bismuth deficient secondary phases such as Fe_2O_3 (α or γ), or Fe_3O_4 as we have previously observed in films grown by PLD at low oxygen partial pressure.[6,7] The lattice constants of the BFO film determined from XRD and electron

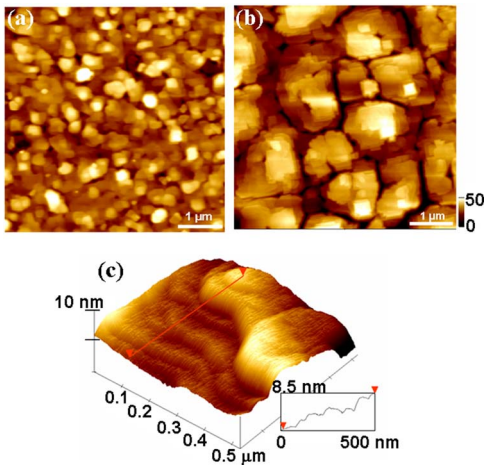

FIG. 2. (Color online) Atomic force microscopy images taken from 5×5 μm^2 areas of BFO thin films grown by (a) conventional PLD and (b) FME method. (c) three-dimensional enhanced image of part of (b) showing atomic steps during growth of the film with grain size of ~2 μm. The inset in (c) is a line scan showing an average step height of 1.2 nm.

diffraction patterns are $a=b=0.394$ nm (in plane) and $c=0.397$ nm (out of plane). These values indicate that the film grown by FME still suffers from some residual compressive strain (–0.9%), originating from the lattice mismatch (–1.15%) between the substrate and the film, even though the film was grown under a quasiequilibrium condition facilitated by the flux.

Figure 4(a) shows the dielectric constant (ε) of BFO thin films grown by the FME method (labeled "FME-BFO") and by standard PLD technique (labeled "PLD-BFO") as a function of frequency. The dissipation factor (tan δ) values of the FME-BFO film and (100) oriented PLD-BFO film were 0.011 ± 0.009 and 0.012 ± 0.01, respectively, in the frequency range of 10 kHz–10 MHz at room temperature. The dielectric constant values of the PLD-BFO thin films varied from 80–130 depending on the frequency and crystalline orientation of the films. These values are slightly higher than the values reported for bulk BFO.[17,18] In contrast, the dielectric constant of FME-BFO films is three times as large (260–340) as that of PLD-BFO films. This may be due to the enhanced crystallinity with the large grain size (~2 μm) in the FME grown films. The leakage current density of FME-BFO thin

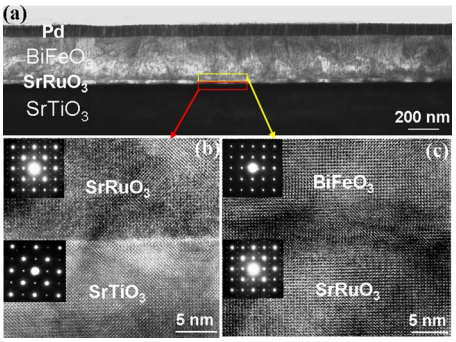

FIG. 3. (Color online) (a) Cross-sectional bright field TEM image showing smooth surface of the BFO film which was grown by FME on SRO buffered (001) oriented STO. 100 nm thick palladium (Pd) was used as top electrode. High resolution lattice images of (b) interface between STO and SRO and (c) interface between SRO and BFO showing epitaxial growth with sharp interfaces. The insets in (b) and (c) are the corresponding diffraction patterns.

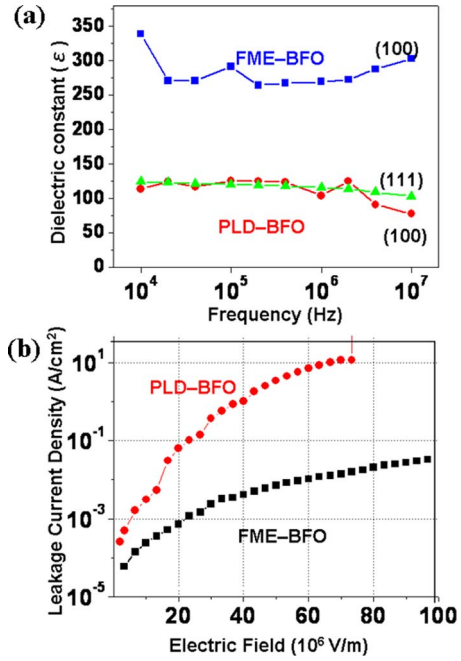

FIG. 4. (Color online) (a) Dielectric constant of BFO thin films fabricated by standard PLD method on STO (100) and (111), and by FME method on STO (100) as a function of frequency. (b) Leakage current density vs electric field curves of BFO thin films fabricated by standard PLD and FME method.

films is also improved by two orders of magnitude compared to that of PLD-BFO films at applied electric fields of up to 100 MV/m, as shown in Fig. 4(b). X-ray photoelectron spectroscopy analysis (not shown here) from a PLD-BFO film did not show any significant amount of Fe^{2+} ions which could explain leakage by double exchange interaction among Fe^{2+}–O^{2-}–Fe^{3+} ions. Therefore, the concentration of Fe^{2+} ions cannot be the dominant reason for the high leakage current in the PLD-BFO films. One possible reason for the leakage current in PLD-BFO films could be the larger fractional area of grain boundary regions in these films, which allow current to pass through with less resistance than in the bulk of the grains. Another possibility is that oxygen vacancies and Bi deficiency in PLD-BFO induce impurity energy levels in the band gap that increase free carrier density by hopping of electrons to these defect levels.[19]

In summary, we improved the crystallinity of BFO films by flux-mediated epitaxy. For the FME growth, we optimized the growth conditions by the combinatorial method. The FME grown films exhibited single crystal quality with large grain size (~2 μm) and a flat surface as well as higher dielectric constant and lower leakage current than films grown by standard PLD.

This work was supported by ONR under Grant Nos. N00014-01-1-0761 and ONR N00014-04-1-0085 and the NSF MRSEC under Grant No. DMR 0520471, NSF DMR 0603644, and ARO W911NF-07-1-0410. This work was also supported by the W. M. Keck Foundation. We acknowledge the use of the TEM in the NISP laboratory and the combinatorial laser molecular beam epitaxy (by Pascal Co., Ltd), shared experimental facilities of our MRSEC.

[1]K. Y. Yun, M. Noda, M. Okuyama, H. Seki, H. Tabata, and K. Saito, J. Appl. Phys. **96**, 3399 (2004).
[2]J. R. Teague, R. Gerson, and W. J. James, Solid State Commun. **8**, 1073 (1970).
[3]Yu. F. Popov, A. M. Kadomtseva, G. P. Vorobev, and A. K. Zvezdin, Ferroelectrics **162**, 135 (1994).
[4]V. A. Murashav, D. N. Rakov, V. M. Ionov, I. S. Dubenko, and Y. U. Titov, Ferroelectrics **162**, 11 (1994).
[5]J. Li, J. Wang, M. Wuttig, R. Ramesh, N. Wang, B. Ruette, A. P. Pyatakov, A. K. Zvezdin, and D. Viehland, Appl. Phys. Lett. **84**, 5261 (2004).
[6]M. Murakami, S. Fujino, S.-H. Lim, B. Varughese, H. Sugaya, T. Hasegawa, S. E. Lofland, L. G. Salamanca-Riba, M. Wuttig, and I. Takeuchi, Appl. Phys. Lett. **88**, 112505 (2006).
[7]S. H. Lim, M. Murakami, W. L. Sarney, S. Q. Ren, A. Varatharajan, V. Nagarajan, S. Fujino, M. Wuttig, I. Takeuchi, and L. Salamanca-Riba, Adv. Funct. Mater. **17**, 2594 (2007).
[8]H. Béa, M. Bibes, A. Barthélémy, K. Bouzehouane, E. Jacquet, A. Khodan, J.-P. Contour, S. Fusil, F. Wyczisk, A. Forget, D. Lebeugle, D. Colson, and M. Viret, Appl. Phys. Lett. **87**, 072508 (2005).
[9]J. F. Scott, C. A. Araujo, B. M. Mclnick, L. D. Mcmillan, and R. Zuleeg, J. Appl. Phys. **70**, 382 (1991).
[10]X. Qi, J. Dho, R. Tomov, M. G. Blamire, J. L. MacManus-Driscoll, Appl. Phys. Lett. **86**, 062903 (2005).
[11]M. Li, A. Kursumovic, X. Qi, and J. L. MacManus-Driscoll, J. Cryst. Growth **293**, 128 (2006).
[12]X. Qi, J. Dho, M. Blamire, Q. Jia, J.-S. Lee, S. Foltyn, and J. L. MacManus-Driscoll, J. Magn. Magn. Mater. **283**, 415 (2004).
[13]R. Takahashi, Y. Yonezawa, M. Ohtani, M. Kawasaki, K. Nakajima, T. Chikyow, H. Koinuma, and Y. Matsumoto, Adv. Funct. Mater. **16**, 485 (2006).
[14]R. Takahashi, Y. Matsumoto, T. Kohno, M. Kawasaki, and H. Koinuma, J. Cryst. Growth **262**, 308 (2004).
[15]R. Takahashi, Y. Yonezawa, M. Ohtani, M. Kawasaki, Y. Matsumoto, and H. Koinuma, Appl. Surf. Sci. **252**, 2477 (2006).
[16]R. Takahashi, Y. Tsuruta, Y. Yonezawa, T. Ohsawa, H. Koinuma, and Y. Matsumoto, J. Appl. Phys. **101**, 033511 (2007).
[17]Yu. E. Rogomskaya, Yu. Ya. Tomashpol'skii, N. Venevtsev, V. M. Petrov, and G. S. Zhdanov, Sov. Phys. JETP **23**, 47 (1966).
[18]M. Mahesh Kumar, V. R. Palkar, K. Srinvas, and S. V. Suryanarayana, Appl. Phys. Lett. **76**, 2764 (2000).
[19]M. Li and J. L. MacManus-Driscoll, Appl. Phys. Lett. **87**, 252510 (2005).